

# Sensitive Fluorescence-Based Thermodynamic and Kinetic Measurements of DNA Hybridization in Solution

Larry E. Morrison\* and Lucy M. Stols

AMOCO Technology Company, P.O. Box 3011, Naperville, Illinois 60566

Received September 18, 1992; Revised Manuscript Received January 19, 1993

**ABSTRACT:** Kinetic and thermodynamic constants associated with DNA hybridization were determined in solution using fluorescence measurements and complementary fluorophore-labeled oligomers. One oligomer was labeled with a 5'-terminal fluorescein, and the other was labeled with a 3'-terminal rhodamine. The juxtaposition of the two labels in double-stranded complexes results in a strong quenching of the fluorescein emission, thereby providing the means for distinguishing single-stranded DNA from double-stranded DNA. Since measurements were based on fluorescence, DNA denaturation and association could be monitored routinely at strand concentrations 100–1000-fold lower than permitted by absorbance hypochromicity measurements. To determine if fluorescence quenching mirrored base pair formation, temperature profiles of DNA association and dissociation were constructed from both absorbance hypochromicity and fluorescence quenching measurements at a number of different DNA concentrations. Analyses of these profiles using the "all-or-none" model of hybridization provided thermodynamic data which were statistically indistinguishable between the two measurement methods, thus validating the use of fluorescence quenching in thermodynamic studies of oligomers. The effects of fluorophore attachment on the thermodynamic properties of the DNA strands were investigated by analyzing the melting curves of different combinations of unlabeled and labeled complementary oligomers. The presence of both labels was found to stabilize the double-stranded DNA by about  $-1.5$  kcal in  $\Delta G^\circ_{298}$ , primarily due to the fluorescein label. Association and dissociation rate constants were determined by fluorescence measurements at different temperatures, and linear Arrhenius plots were obtained. The fluorescence measurements provided a unique "label dilution" method for measuring dissociation rate constants of oligomers based upon the dynamic association and dissociation of complementary DNA strands at constant temperature. Association rate measurements were simplified since relatively low concentrations of complementary oligomers could be mixed, thereby reducing hybridization rates and eliminating the need for rapid mixing and measurement techniques.

Reversible hybridization of complementary polynucleotides is fundamental to the biological processes of replication, transcription, and translation. Physical studies of nucleic acid hybridization are necessary for understanding these important biological processes on a molecular level. In addition to understanding natural processes, the physical characterization of nucleic acid hybridization is important for predicting the behavior of nucleic acids in vitro, for example, in hybridization assays used to detect specific polynucleotide sequences. With a knowledge of hybridization enthalpies, entropies, and rate constants, optimal assay conditions, such as temperature, hybridization equilibration times, and DNA reagent size, can be calculated instead of determined through extensive experimentation.

Physical studies of nucleic acid hybridization in solution require the ability to separately monitor paired and unpaired nucleic acids. Nucleic acid hybridization in solution may be monitored by several methods which include absorbance spectroscopy [hypochromicity and circular dichroism (CD);<sup>1</sup> Bush, 1974], calorimetry (Breslauer, 1986), and nuclear magnetic resonance (NMR; Patel et al., 1982). All of these techniques, however, require relatively large amounts of nucleic acids, milligram quantities for NMR and calorimetry and microgram or greater quantities for absorbance and CD

measurements. Often nucleic acids of interest are not available in such quantities. Radioactivity measurements allow the detection of minute amounts of radioisotope-labeled DNA; however, true solution-phase measurements are not possible since physical separation of hybridized and unhybridized nucleic acids is required, either by precipitation, by immobilization, or by chromatographic means. Separation techniques not only perturb the hybridization equilibria under study but also rule out the possibility of continuously monitoring hybridization with time.

Fluorescence measurements offer a considerably more sensitive measure of nucleic acid concentration than the conventional solution-phase detection techniques. In addition, the sensitivity of fluorophores to their environments offers a means by which to distinguish hybridized from unhybridized nucleic acids without resorting to separation techniques. This was first demonstrated by attaching different fluorescent labels to the termini of oligonucleotides which hybridize to adjacent regions on a complementary strand of DNA (Heller & Morrison, 1985). Proper selection of the fluorophores led to detectable energy transfer between the labels upon hybridization of the two labeled strands to the third strand. Similar experiments have been reported since (Cardullo et al., 1988).

We have been particularly interested in using energy transfer and fluorescence quenching to study the hybridization between two fluorophore-labeled complementary DNA strands, as shown in Figure 1. Attaching fluorescent labels ( $F_1$  and  $F_2$  in Figure 1) to the respective 3'- and 5'-termini of complementary DNA strands, we observed strong quenching interactions between particular fluorophore pairs upon hybrid-

<sup>1</sup> Abbreviations: CD, circular dichroism; NMR, nuclear magnetic resonance; DNA, deoxyribonucleic acid; TDT, terminal deoxynucleotidyl transferase; BSA, bovine serum albumin; 10-mer, 10-nucleotide-long DNA oligomer; 20-mer, 20-nucleotide-long DNA oligomer; FL, fluorescein label appended to DNA oligomer; TR, Texas Red label appended to DNA oligomer; FITC, fluorescein isothiocyanate.

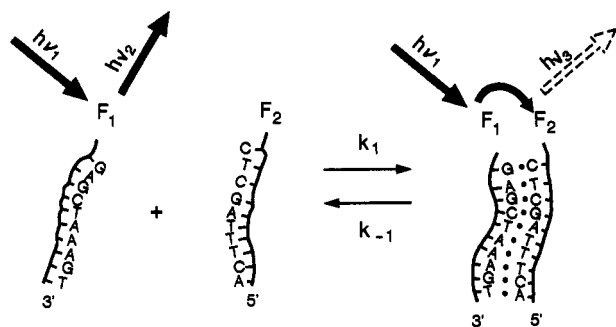


FIGURE 1: Scheme showing the dynamic equilibrium between complementary labeled polynucleotides and the interaction between terminal labels. One polynucleotide is labeled on its 5'-terminus with a fluorophore,  $F_1$ , that is sensitive to the proximity of a label,  $F_2$ , attached to the 3'-terminus of the complementary strand. When the labels are far apart, as in the single-stranded state,  $F_1$  emits characteristic light of energy  $h\nu_2$  following excitation with light of energy  $h\nu_1$ . When hybridization brings the two labels close to one another, interaction between the labels quenches the fluorescence of  $F_1$ , either degrading the energy absorbed by  $F_1$  to heat or, in the case of energy transfer between the two labels, causing light of energy  $h\nu_3$  to be emitted from  $F_2$ .

ization (Morrison, 1987, 1992; Morrison et al., 1989). Competitive hybridizations between the labeled and unlabeled DNA strands proved to be the basis of a completely homogeneous (solution-phase only) DNA hybridization assay. The same labeling strategy should also provide the means for determining any physical constants relating to the hybridization process depicted in Figure 1. True solution-phase measurements, therefore, are possible at the low DNA concentrations afforded by fluorescence measurements. In fact, we reported thermal profiles of DNA base pairing (melting curves) monitored by fluorescence quenching at oligomer concentrations 1000-fold lower than was possible using absorbance measurements (Morrison et al., 1989).

With the attachment of fluorescent labels, however, come the questions of how does the hybridization process affect the labels and how do the labels affect the hybridization process. If thermodynamic values are to be extracted from fluorescence melting curves, we must know if the fluorescence changes of the labels are proportional to the number of base pairs formed. Once thermodynamic values have been determined, we would like to know how these values have been altered by the presence of the label. In this paper, DNA melting curves recorded by both fluorescence measurements and absorbance hypochromicity measurements are quantitatively compared. Two complementary pairs of deoxyoligonucleotides are used: one pair of 10 nucleotides length (referred to as 10-mers) and one pair of 20 nucleotides length (referred to as 20-mers). Each pair contains a 5'-fluorescein-labeled strand and a 3'-rhodamine (Texas Red)-labeled strand. Melting curves recorded on the labeled oligomers, as well as combinations of labeled and unlabeled oligomers, are used to determine melting curve midpoints ( $T_m$  values), enthalpy changes, entropy changes, and free energy changes associated with hybridization. Comparisons among these data sets allow conclusions to be drawn relevant to the questions of fluorescent label participation in the hybridization process. In addition, the same fluorescent methods are used for kinetic measurements of DNA hybridization. In this context, simplification of experimental design as well as increased sensitivity is examined.

## MATERIALS AND METHODS

**Chemicals.** Fluorescein 5'-isothiocyanate (FITC) and Texas Red (sulfonic acid chloride derivative of sulforhodamine

101) were purchased from Molecular Probes, Inc. (Eugene, OR). Terminal deoxynucleotidyl transferase (TDT) was purchased from Life Sciences (St. Petersburg, FL) and Supertechs (Bethesda, MD). T4 polynucleotide kinase and  $\lambda$  phage DNA were purchased from New England Biolabs (Beverly, MA). Nuclease-free bovine serum albumin (BSA) was purchased from GIBCO BRL (Gaithersburg, MD). 8-[(6-Aminoethyl)amino]adenosine 5'-triphosphate and buffer salts were purchased from Sigma Chemical Co. (St. Louis, MO). Phosphoramidite reagents for DNA synthesis were purchased from Applied Biosystems (Foster City, CA). High-purity NaCl for buffers used in fluorescence measurements was either J. T. Baker Chemical Co. (Phillipsburg, NJ) ULTREX grade or Johnson Matthey PURATRONIC grade distributed by Alfa Products (Danvers, MA).

**Preparation and Labeling of DNA.** The complementary 10-mers, d(TTGGTGATCC) and d(GGATCACCAA), and the complementary 20-mers, d(AGATTAGCAGGTTCCACC) and d(GGTGGGAAACCTGCTAATCT), were synthesized using an Applied Biosystems Model 380B DNA automated synthesizer using protocols supplied by Applied Biosystems. The oligomers were purified by liquid chromatography performed on a Pharmacia (Piscataway, NJ) low-pressure chromatography FPLC system containing a Model LCC-500 liquid chromatography controller and two Model P-500 pumps. 20-mers were purified on Pharmacia ProRPC and PepRPC reverse-phase columns using a linear acetonitrile gradient which started at 1% acetonitrile/99% 10 mM triethylammonium acetate, pH 7.0, and was changed to 18% acetonitrile/82% 10 mM triethylammonium acetate, pH 7.0, at a rate of 0.4% acetonitrile/min and a flow rate of 2 mL/min. 10-mers were purified on a Pharmacia Mono Q anion-exchange column using a linear gradient which started at 30% methanol/70% 0.05 M  $\text{KH}_2\text{PO}_4$ , pH 7.0, and was changed to 30% methanol/70% 0.05 M  $\text{KH}_2\text{PO}_4$ , 1 M  $(\text{NH}_4)_2\text{SO}_4$ , pH 7.0, at a rate of 0.01 M  $(\text{NH}_4)_2\text{SO}_4$ /min and a flow rate of 1 mL/min.

5'- and 3'-terminal labeling was performed as described previously (Morrison et al., 1989; Morrison, 1992). 5'-Labeling was accomplished by reacting ethylenediamine with a 5'-phosphorylated oligomer (Chu et al., 1983) to provide a 5'-aliphatic amine group which was further reacted with FITC to provide a 5'-fluorescein label (FL). For 3'-labeling, 8-[(6-aminoethyl)amino]adenosine triphosphate was coupled to the 3'-terminus of an oligomer in a TDT-catalyzed reaction. Texas Red was then reacted with the aminoethyl substituent of the 3'-[(6-aminoethyl)amino]adenosine to introduce a 3'-sulforhodamine 101 label (TR) onto the oligomer. Labeled oligomers were purified on the FPLC system using a ProRPC column and a linear acetonitrile gradient which started at 1% acetonitrile/99% 10 mM triethylammonium acetate, pH 7.0, and was changed to 50% acetonitrile/50% 10 mM triethylammonium acetate, pH 7.0, at a rate of 1.0% acetonitrile/min at a flow rate of 2 mL/min.

**Absorbance Measurements.** Absorbance spectra were recorded using a Hewlett-Packard Model 8451A diode array spectrophotometer (Palo Alto, CA). Concentrations of unlabeled oligomers were calculated from the absorbance at 260 nm ( $A_{260}$ ), and extinction coefficients were determined using the nearest-neighbor approximation and published values of mono- and dinucleotides (Borer, 1976). Concentrations of labeled oligomers were calculated from the  $A_{260}$  using the following extinction coefficients reported previously (Morrison et al., 1989):  $(1.02 \pm 0.17) \times 10^5 \text{ M}^{-1} \text{ cm}^{-1}$  for 5'-FL-d(TTGGTGATCC),  $(2.07 \pm 0.25) \times 10^5 \text{ M}^{-1} \text{ cm}^{-1}$  for 5'-

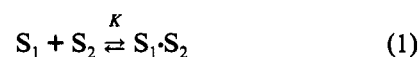
FL-d(AGATTAGCAGGTTTCCCACC),  $(1.34 \pm 0.23) \times 10^5 \text{ M}^{-1} \text{ cm}^{-1}$  for d(GGATCACCAA)-TR-3', and  $(2.28 \pm 0.27) \times 10^5 \text{ M}^{-1} \text{ cm}^{-1}$  for d(GGTGGGAAACCT-GCTAATCT)-TR-3'. Absorbance hypochromicity measurements and automated melting curves were recorded by monitoring  $A_{260}$ , as described previously (Morrison et al., 1989; Morrison, 1992), on solutions containing the complementary DNA oligomers in 1 M NaCl/10 mM  $\text{NaH}_2\text{PO}_4$ , pH 8.0. Melting curves were recorded by starting at a temperature well above the  $T_m$  and linearly reducing the temperature at a rate of  $10^\circ\text{C/h}$  to a temperature well below the  $T_m$  (association segment). The temperature was then raised at the same rate until the starting temperature was reached again (dissociation segment). Absorbance values were continuously recorded and averaged within  $0.1^\circ\text{C}$  increments.

**Fluorescence Measurements.** Fluorescence measurements were performed on an SLM Model 4800 spectrofluorometer (Champaign, IL) modified for photon counting detection and automated for recording fluorescence versus temperature or time. The modifications, automation, and procedures are described elsewhere (Morrison et al., 1989; Morrison, 1992). All melting curves were recorded on solutions containing the complementary DNA oligomers in 1 M NaCl/10 mM  $\text{NaH}_2\text{PO}_4$ , pH 8.0. Fluorescein was excited at 495 nm (2–4-nm slit width), and the emission was measured through a three-cavity interference filter passing a band of light centered at 520 nm with an 8-nm full width at half-maximum (Ditric Optics, Inc., Hudson, MA). Melting curves were recorded by starting at a temperature well above the  $T_m$  and linearly reducing the temperature well below the  $T_m$  (association segment). The temperature was then raised at the same rate until the starting temperature was reached again (dissociation segment). Fluorescence values were continuously recorded and averaged within  $0.1^\circ\text{C}$  increments. The temperature scan rates were  $10^\circ\text{C/h}$  except for melting curves recorded at oligomer concentrations below 10 nM where the scan rates were reduced to  $3\text{--}5^\circ\text{C/h}$  to reduce hysteresis resulting from slower hybridization rates. DNA association and dissociation rates were measured by equilibrating one or more oligomer strands in 1.75 mL of buffer (1 M NaCl/10 mM  $\text{NaH}_2\text{PO}_4$ , pH 8.0) in a cuvette placed in the fluorometer's thermostated sample compartment and then injecting  $50 \mu\text{L}$  of buffer containing the remaining oligomer(s) to initiate the reaction. Fluorescence values were continuously recorded starting prior to the injection and extending until the reaction was nearly complete;  $5\text{--}10 \mu\text{g/mL}$   $\lambda$  phage DNA was included in dilute samples of the 10-mer and 20-mer DNA ( $<0.1 \mu\text{M}$ ) to serve as a carrier and block adsorptive losses of the oligomers.

For all fluorescence measurements, fluorescence quenching due to collisions between fluorophores on unhybridized strands was estimated to be less than 0.1%. This was calculated using a biomolecular rate constant for quenching of  $1 \times 10^{10} \text{ M}^{-1} \text{ s}^{-1}$  (the largest possible value in aqueous solution; Lakowicz, 1983), a 4-ns fluorescein fluorescence lifetime, and the highest oligomer concentrations used in this work ( $<30 \mu\text{M}$ ).

**Analysis of Thermodynamic Data.** The thermodynamic analyses were based upon  $T_m$  values derived from melting curve recordings. The  $T_m$  values were determined by fitting the absorbance or fluorescence versus temperature data with the predicted temperature dependence derived by assuming the "all-or-none" model for oligomer hybridization (Applequist & Damle, 1963, 1965). Given two complementary strands of DNA,  $S_1$  and  $S_2$ , the "all-or-none" model considers the existence of only completely base-paired,  $S_1 \cdot S_2$ , and completely single-stranded DNA, according to the equilibrium represented

by eq 1 and 2 where  $K$  is the equilibrium constant. The fraction



$$K = [S_1 \cdot S_2] / [S_1][S_2] \quad (2)$$

of the total number of nucleotides bonded to opposing complementary nucleotides (base paired),  $f$ , as a function of  $K$  is then given by eq 3 where  $[S_1]_0$  and  $[S_2]_0$  are the total

$$f \equiv [S_1 \cdot S_2] / [S_1]_0 = \{1 + [S_1]_0(1 + r)K - [1 + 2[S_1]_0(1 + r)K + K^2[S_1]_0^2(r - 1)^2]^{0.5}\} (2[S_1]_0 K)^{-1} \quad (3)$$

concentrations of each strand ( $[S_1]_0 = [S_1] + [S_1 \cdot S_2]$ ,  $[S_2]_0 = [S_2] + [S_1 \cdot S_2]$ ), and we have generalized the equation to accommodate complementary oligomers at different concentrations by assigning  $r$  equal to the ratio of the total strand concentrations,  $[S_2]_0/[S_1]_0$ . Substituting  $\exp(\Delta S^\circ/R - \Delta H^\circ/RT)$  for  $K$  then provides  $f$  in terms of  $\Delta H^\circ$ ,  $\Delta S^\circ$ , and the absolute temperature,  $T$ , where  $\exp(X) \equiv e^X$ .

The dependencies of the measured quantities  $A_{260}$  and the fluorescence,  $F$ , on  $f$  are given by eq 4 and 5, respectively,

$$A_{260} = [S_1]_0 \{(\epsilon_{260,S_1} + \epsilon_{260,S_2})(1 - f) + (\epsilon_{260,S_1 \cdot S_2})f + (r - 1)\epsilon_{260,S_2}\} \quad (4)$$

$$F = \Psi[S_1]_0 \{\Phi_{S_1}(1 - f) + \Phi_{S_1 \cdot S_2}f\} = \Psi[S_1]_0 \{\Phi_{S_1} + (\Phi_{S_1 \cdot S_2} - \Phi_{S_1})f\} \quad (5)$$

where  $\epsilon_{260,S_1}$ ,  $\epsilon_{260,S_2}$ , and  $\epsilon_{260,S_1 \cdot S_2}$  are the absorbance extinction coefficients for  $S_1$ ,  $S_2$ , and  $S_1 \cdot S_2$ , respectively,  $\Psi$  is a sensitivity factor which includes the rate of light absorption by the fluorophore and the instrument efficiency of detecting light at the wavelengths emitted by the fluorophore, and  $\Phi_{S_1}$  and  $\Phi_{S_1 \cdot S_2}$  are the fluorescence quantum yields of the fluorophore attached to  $S_1$  when  $S_1$  is single stranded and hybridized to  $S_2$ , respectively. Equation 5 was derived for the condition in which the fluorophore being monitored, fluorescein in these studies, is attached to the strand in limiting concentration,  $S_1$ . If the fluorescein were attached to the strand in excess,  $F$  would be increased by a constant amount equal to  $\Psi\Phi_{S_1}(1/r - 1)[S_1]_0$ .

The method of nonlinear least squares (Marquadt's method implemented by the Hewlett Packard Statistics Library for the Model HP9836 computer) was used to obtain values for the parameters in eq 4 and 5 which best fit the absorbance versus temperature and fluorescence versus temperature data in the melting curves. Five parameters were used in each fitting operation representing  $\Delta H^\circ$ ,  $\Delta S^\circ$ , a constant (representing the last term in eq 4 and a constant background fluorescence not included in eq 5), and either  $\epsilon_{260,S_1} + \epsilon_{260,S_2}$  and  $\epsilon_{260,S_1 \cdot S_2}$  in eq 4 or  $\Psi\Phi_{S_1}$  and  $\Psi\Phi_{S_1 \cdot S_2}$  in eq 5. The data from each association and dissociation segment were fit separately, and the parameters from the best fits were used to calculate  $T$  at  $f = 0.5$  for each segment. The average of the two segment values was assigned to the  $T_m$  of that melting curve.  $1/T_m$  values were plotted versus  $\log [S_1]_0$  for each pair of oligomers, and  $\Delta H^\circ$  and  $\Delta S^\circ$  values were determined from the slopes and intercepts of each least-squares line through the various data sets, according to eq 6 where  $R$  is the gas constant, and eq 6 has been derived for the general case where concentrations of the complementary strands may not be equal

$$([S_1]_0 \leq [S_2]_0, r = [S_2]_0/[S_1]_0).$$

$$1/T_m = 2.303R \log[S_1]_0/\Delta H^\circ + [\Delta S^\circ + 2.303R \log(r - 0.5)]/\Delta H^\circ \quad (6)$$

Comparisons of any two  $1/T_m$  versus  $\log[S_1]_0$  data sets were performed by multiple linear regression analysis using the fitted regression equation:  $1/T_m = a_1 + a_2Z + (b_1 + b_2Z) \log[S_1]_0$ , where  $Z = 1$  for one data set and  $Z = 0$  for the other data set. To determine if the parameters differed between the two data sets, the joint hypothesis  $a_2 = 0$  and  $b_2 = 0$  was tested using the SAS (Cary, NC) statistical package.

Ninety percent confidence intervals for  $\Delta H^\circ$  and  $\Delta S^\circ$  were obtained using  $\Delta H^\circ$  and  $\Delta S^\circ$  as fitting parameters in nonlinear least-squares analyses of the  $1/T_m$  versus  $\log[S_1]_0$  data sets. Values of  $\Delta G^\circ_{298}$  were calculated from the relationship  $\Delta G^\circ_{298} = \Delta H^\circ - 298\Delta S^\circ$ , and confidence intervals for  $\Delta G^\circ_{298}$  were determined as the confidence intervals of the intercepts of  $\Delta G^\circ$  versus  $T - 298$  data analyzed by linear regression.

**Analysis of Kinetic Data.** The kinetic analyses were performed by determining  $k_1$  and  $k_{-1}$  from nonlinear least-squares fits of integrated rate equations to the fluorescence versus time data. For dissociation curves, recorded using the label dilution technique, only the dissociation of labeled strands is detectable, and the data were fit with equation 5, where  $f$  is determined by eq 7 according to the first-order decay law with  $t$  representing time. Three fitting parameters were used representing  $k_{-1}$ ,  $\Psi[S_1]_0\Phi_{S1}$ , and  $\Psi[S_1]_0(\Phi_{S1S2} - \Phi_{S1})$ .

$$f = \exp(-k_{-1}t) \quad (7)$$

For association curves,  $f$  in eq 5 was determined by the integrated rate equation for the bimolecular reaction between  $S_1$  and  $S_2$ , both added as single strands at  $t = 0$ , and given by eq 8 where  $\alpha = -k_{-1}/k_1 - (r + 1)[S_1]_0$ ,  $\beta = \{(k_{-1}/k_1)^2 +$

$$f = \frac{\exp(\beta k_1 t) - 1}{2[S_1]_0\{(\alpha - \beta)^{-1} - (\alpha + \beta)^{-1} \exp(\beta k_1 t)\}} \quad (8)$$

$2(k_{-1}/k_1)(r + 1)[S_1]_0 + (1 - r)^2[S_1]_0^2\}^{0.5}$ , and  $r$  is defined as above. To simplify fitting, the values of  $k_{-1}$  were first determined from the dissociation rate versus temperature data and entered as constants in eq 8, reducing the number of fitting parameters to 3.

Activation energies,  $E_{act.}$ , and collision factors,  $A$ , were determined by linear least-squares analysis of the  $\ln(k_1)$  or  $\ln(k_{-1})$  versus  $1/T$  data according to the Arrhenius equation:

$$\ln(k) = \ln(A) - E_{act.}/RT \quad (9)$$

## RESULTS

**DNA Melting Curves by Fluorescence and Absorbance.** Melting curves were recorded on solutions containing approximately equimolar amounts of complementary DNA oligomers ( $r = 1.01$ – $1.14$ ) at different concentrations in buffer containing 1 M NaCl and 10 mM  $\text{NaH}_2\text{PO}_4$  at pH 8.0. The melting curves were generally comprised of two portions, a portion recorded while the temperature was decreased (the association segment) and a portion recorded while the temperature was increased (the dissociation segment). The oligomers were either 10-mers (5'-TTGGTGATCC and its complement) or 20-mers (5'-AGATTAGCAGGTTTC-CCACC and its complement). Melting curves were recorded for combinations of labeled and unlabeled oligomers. When labeled, 5'-TTGGTGATCC contained a single FITC label attached to the 5'-terminus. The complementary oligomer contained a single Texas Red label attached to its 3'-terminus.

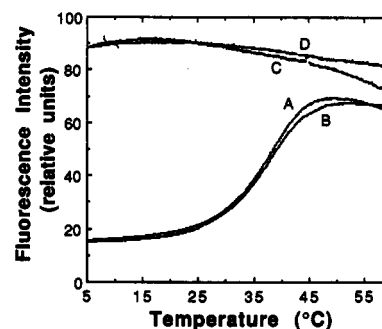


FIGURE 2: Fluorescence melting curves for the complementary labeled 10-mer pair (A and B) and a single fluorescein-labeled strand (C and D) in 1 M NaCl/10 mM  $\text{NaH}_2\text{PO}_4$ , pH 8.0. The 10-mer pair was formed from two complementary DNA strands, one containing a 5'-fluorescein label and the other containing a 3'-Texas Red label, each strand present at 27 nM. Only the fluorescein-labeled strand was used in recording data sets C and D. The solutions were equilibrated at the high-temperature extreme before linearly decreasing the temperature to the low-temperature extreme at a rate of  $10^\circ\text{C}/\text{h}$  (A and C). The temperature was then increased at the same rate to the high-temperature extreme (B and D).

Likewise, when labeled, 5'-AGATTAGCAGGTTTC-CCACC contained a single FITC label on its 5'-terminus, and its labeled complement contained single Texas Red label on its 3'-terminus. Melting curves were monitored by absorbance when only one or neither of the complementary oligomers were labeled. When both complementary 10-mer strands were labeled, the melting curves were recorded by monitoring both FITC fluorescence and  $A_{260}$ . The absorbance and fluorescence melting curves were recorded on the same samples 1 day apart when within the concentration range of the absorbance measurements. Additional fluorescence melting curves were recorded outside the concentration range of the absorbance measurements. Labeled 20-mers were monitored by fluorescence only.

Typical fluorescence melting curves are displayed in Figure 2 for the labeled 10-mer pair present at 27 nM. Data set A forms the association segment of the curve, and data set B forms the dissociation segment. The dissociation portion of the melting curve nearly retraces the association portion; however, some hysteresis is apparent, particularly in the high-temperature region. To investigate the hysteresis further, FITC fluorescence was recorded using solutions containing only the FITC-labeled strand, while the temperature was decreased and then increased in the same manner as for the solutions containing complementary DNA strands. The association segment (C) and dissociation segment (D) of the single-strand data are also plotted in Figure 2, and show a hysteresis in the high-temperature region similar to the complementary DNA strands. Since this indicates the high-temperature hysteresis may be primarily due to FITC on the single-stranded DNA, the temperature dependence of the single strand was used to correct the fluorescence data of the double-stranded oligomers. The single-strand data sets were first fit with polynomial functions and normalized to values of 1 at their respective maxima. The fluorescence values in data sets A and B were then divided by the corresponding values of the fitted and normalized data sets C and D, respectively. The resulting corrected melting curves for the complementary 10-mers are plotted in Figure 3, together with the nonlinear least-squares fits of the combined eq 3 and 5 which were used to determine the  $T_m$  values for association and dissociation segments of the data. All four curves were offset and scaled before plotting in order to express the temperature dependence of the fluorescence as the percentage

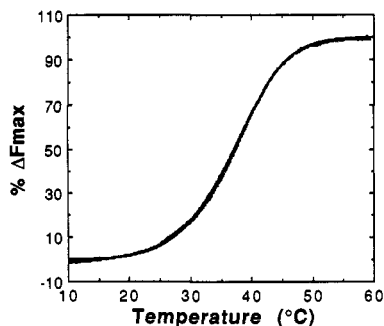


FIGURE 3: Corrected fluorescence melting curves of the labeled complementary 10-mer pair at 27 nM. The melting curve plotted in Figure 2 (data sets A and B) for the complementary labeled pair of 10-mers was corrected using the temperature dependence of the single fluorescein-labeled strand, also plotted in Figure 2 (data sets C and D). The corrected fluorescence values were offset and scaled to provide  $\% \Delta F_{\max}$  as defined in eq 10. Also plotted are the best fits of eq 5 to the corrected data sets A and B. Identifying labels were not included in the graph since neither the corrected data sets nor the fitting lines can be distinguished due to the removal of hysteresis by the correction procedure.

of the maximum fluorescence change,  $\% \Delta F_{\max}$ , which, in light of eq 5, is equivalent to the percentage of the complementary strands which are unhybridized at  $T$ :

$$\% \Delta F_{\max} = 100(F_T - F_{T \ll T_m}) / (F_{T \gg T_m} - F_{T \ll T_m}) = 100(1 - f) \quad (10)$$

where  $F_T$  is the fluorescence  $F$  measured at  $T$ ,  $F_{T \ll T_m}$  is  $F$  measured at a temperature well below the  $T_m$  such that  $f$  is essentially 1, and  $F_{T \gg T_m}$  is  $F$  measured at a temperature well above the  $T_m$  such that  $f$  is essentially 0. Following the offsetting and scaling procedure, both data sets and the two fitted curves show nearly complete correspondence, as can be seen in Figure 3 where the two data sets and fitted curves cannot be distinguished separately.

Thermodynamic information was derived from the concentration dependence of fluorescence melting curves in a manner analogous to that used conventionally for absorbance melting curves [e.g., see Breslauer (1986)]. Fluorescence and absorbance  $1/T_m$  versus  $\log[S]_0$  plots for the various combinations of labeled and unlabeled 10-mers and 20-mers are presented in Figure 4. Fluorescence data for the labeled 10-mers are represented by open squares while the corresponding absorbance data are represented by closed squares. Absorbance data derived from absorbance melting curves of 10-mers with only the fluorescein label or the Texas Red label present are represented by the open circles and closed triangles, respectively. Absorbance data for unlabeled 10-mers are represented by open triangles. The corresponding data derived from fully labeled 20-mers using fluorescence measurements and unlabeled 20-mers using absorbance measurements are represented by closed circles and crosses, respectively.

The fluorescence data presented in Figure 4 were derived from melting curves corrected for the temperature dependence of the fluorescein label, as described above. Similar data were derived from the uncorrected melting curves and statistically compared with the corrected data to determine if the added correction procedure had a significant effect on the  $T_m$  values determined from the melting curves. Significance levels for no difference between the corrected and uncorrected data sets were 0.82 and 0.96 for the labeled 10-mers and labeled 20-mers, respectively. In general, a significance level of 0.05 or lower is required to reject the hypothesis of no statistical difference between the two data sets being compared; therefore,

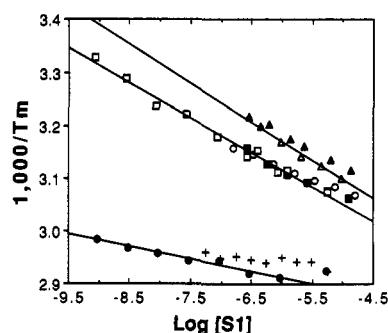


FIGURE 4: Absorbance and fluorescence melting curve data for several series of melting curves using different combinations of labeled and unlabeled 10-mer and 20-mer pairs of complementary oligonucleotides in 1 M NaCl/10 mM NaH<sub>2</sub>PO<sub>4</sub>, pH 8.0. Values of  $r$  were between 1.01 and 1.14. The different combinations of complementary oligomers used for recording melting curves by either method were 5'-FL-10-mer + 10-mer-TR-3' (absorbance data represented by closed squares, fluorescence data represented by open squares), 5'-FL-10-mer + unlabeled 10-mer (absorbance data represented by open circles), unlabeled 10-mer + 10-mer-TR-3' (absorbance data represented by closed triangles), unlabeled 10-mer + unlabeled 10-mer (absorbance data represented by open triangles), 5'-FL-20-mer + 20-mer-TR-3' (fluorescence data represented by closed circles), and unlabeled 20-mer + unlabeled 20-mer (absorbance data represented by crosses). The first 10-mer listed in each combination is 5'-d(TTGGTGATCC), and the second 10-mer is the complement. The first 20-mer listed in each combination is 5'-d(AGATTAGCAG-GTTTCCACC), and the second 20-mer is the complement.

correction of the melting curves did not significantly alter the  $T_m$  values.

In a similar manner, absorbance and fluorescence data collected on the same labeled 10-mers were compared to determine if fluorescence quenching changes with temperature provided the same thermodynamic information as absorbance hypochromicity changes with temperature. The significance level for no difference between the fluorescence and absorbance data was 0.30, therefore indicating no statistical difference between the two data sets. It may be added that the significance levels for comparisons between the slopes and intercepts of the corrected versus uncorrected and fluorescence versus absorbance data sets were also all well above 0.05, indicating that the values of parameters derived from the slopes and intercepts, i.e.,  $\Delta H^\circ$  and  $\Delta S^\circ$ , were not significantly different.

The three lines drawn through the data in Figure 4 are linear least-squares fits to the unlabeled 10-mer data, the labeled 10-mer data, and the labeled 20-mer data. Since the absorbance and fluorescence data derived from the labeled 10-mers were not significantly different, both data sets were used in calculating the least-squares line through the labeled 10-mer data. The slopes and intercepts of these lines were used to calculate  $\Delta H^\circ$ ,  $\Delta S^\circ$ , and  $\Delta G^\circ_{298}$  for the single-strand-to-double-strand transitions of each data set plotted in Figure 4 (least-squares lines not shown for all). These data are compiled in Table I for each of the labeled and unlabeled oligomer combinations tested.

In addition to  $T_m$  values, the widths of the transition regions in fluorescence and absorbance melting curves were compared by measuring the temperature difference,  $\Delta t$ , between the 10% and 90% hybridization points on both the association and dissociation segments. The resulting data are listed in Table II for melting curves recorded on solutions of 1.24 and 5.54  $\mu$ M labeled 10-mer pairs.

**Kinetics of DNA Association and Dissociation.** The same labeled 10-mers and 20-mers were used to record strand association and dissociation rates. Figure 5 shows an example

Table I: Thermodynamic Values Determined from Absorbance- and Fluorescence-Based Melting Curves of 10- and 20-mers<sup>a</sup>

oligomer	detection method <sup>b</sup>	$\Delta H^\circ$ (kcal/mol)	$\Delta S^\circ$ (cal mol <sup>-1</sup> K <sup>-1</sup> )	$\Delta G^\circ_{298}$ (kcal/mol)	$\Delta G^\circ_{298, \text{pred}}$ (kcal/mol) <sup>c</sup>
10-mer/10-mer	absorbance	-62 ± 11	-169 ± 36	-11.96 ± 0.45	-12.9
10-mer/10-mer-TR	absorbance	-72.9 ± 8.2	-204 ± 26	-12.07 ± 0.30	
FL-10-mer/10-mer	absorbance	-100.9 ± 8.4	-286 ± 26	-15.51 ± 0.41	
FL-10-mer/10-mer-TR	absorbance	-82 ± 18	-226 ± 55	-14.06 ± 0.86	
	fluorescence				
	uncorrected	-70.7 ± 8.8	-192 ± 28	-13.36 ± 0.33	
	corrected	-69.5 ± 7.0	-188 ± 22	-13.38 ± 0.27	
	combined	-71.6 ± 5.0	-195 ± 16	-13.46 ± 0.22	
20-mer/20-mer	absorbance	-380 ± 260	-1100 ± 780	-40 ± 14	-33.0
FL-20-mer/20-mer-TR	fluorescence				
	uncorrected	-196 ± 51	-540 ± 150	-33.5 ± 4.0	
	corrected	-194 ± 48	-540 ± 140	-33.3 ± 3.8	

<sup>a</sup> Uncertainties listed with the thermodynamic values are the 90% confidence intervals determined by regression analysis as described under Materials and Methods. <sup>b</sup> Thermodynamic values were determined from fluorescence data sets before and after correction for the temperature dependence of the FL-10-mer fluorescence, as indicated. <sup>c</sup> Predicted values of the standard free energy change,  $\Delta G^\circ_{298, \text{pred}}$ , were calculated from nearest-neighbor interactions according to Bresslauer et al. (1986).

Table II: Temperature Difference,  $\Delta t$ , between 10% and 90% Hybridization Points

measurement method	$[S_1]_0$ ( $\mu\text{M}$ )	melting curve segment	$\Delta t$ (°C)
absorbance	5.54	dissociation	18.2
absorbance	5.54	association	16.0
fluorescence	5.54	dissociation	16.5
fluorescence	5.54	association	16.2
absorbance	1.24	dissociation	17.7
absorbance	1.24	association	16.2
fluorescence	1.24	dissociation	16.2
fluorescence	1.24	association	15.9

of an association and dissociation curve monitored by fluorescence. The collection of data points comprising the association curve was recorded by monitoring the fluorescence of the fluorescein label with time after injecting a small concentrated solution of the 3'-TR-labeled 10-mer into a larger solution of the complementary 5'-fluorescein-labeled 10-mer equilibrated at a reaction temperature of 16.2 °C. The solid line drawn through the set of points was calculated as the best fit of the integrated second-order rate equation to the data. The dissociation data set in Figure 5 was obtained by measuring the fluorescence of the fluorescein label with time after injecting a small concentrated solution of one of the unlabeled 10-mers into a larger solution containing approximately equimolar concentrations of the complementary labeled 10-mers equilibrated at 32.0 °C (method 1). The amount of unlabeled 10-mer injected was 100-fold larger than the amount of either labeled strand. The line drawn through the dissociation data was calculated as the best fit of the integrated first-order rate equation to the data. Dissociation curves were also recorded by injecting a small concentrated solution of the complementary labeled strands into a larger solution of excess unlabeled 10-mer equilibrated at the reaction temperature (method 2, data not shown in Figure 5). Rate constants determined by both methods were in good agreement.

Dissociation rate curves were recorded using different concentrations of the excess unlabeled oligomer in order to determine whether the observed dissociation kinetics were first-order or pseudo-first-order. Data were collected by both method 1 and method 2 using 10 nM concentrations of the labeled oligomers. The dissociation rate constants determined at 30.5 °C for each method at each concentration of the unlabeled DNA strand are listed in Table III.

The temperature dependencies of the 10-mer and 20-mer association and dissociation reactions were examined by recording association and dissociation curves at a number of

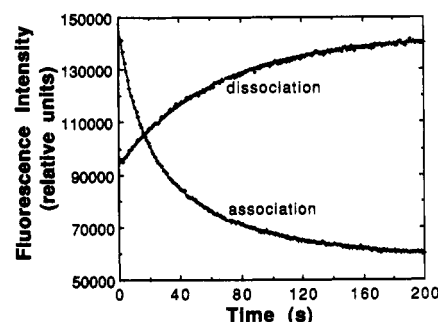


FIGURE 5: Association and dissociation of 5'-FL-d(TTGGTGATCC) and d(GGATCACCAA)-TR-3' with time as measured by the fluorescence of the fluorescein label. Association was initiated by injecting 18 pmol of d(GGATCACCAA)-TR-3' in 50  $\mu\text{L}$  of 1 M NaCl/10 mM NaH<sub>2</sub>PO<sub>4</sub>, pH 8.0, into a cuvette containing 18 pmol of 5'-FL-d(TTGGTGATCC) and 9  $\mu\text{g}$  of  $\lambda$  phage DNA in 1.75 mL of the same buffer pre-equilibrated at 32.0 °C. Dissociation was initiated by injecting 1.8 nmol of d(TTGGTGATCC) in 50  $\mu\text{L}$  of 1 M NaCl/10 mM NaH<sub>2</sub>PO<sub>4</sub>, pH 8.0, into a cuvette containing 18 pmol of 5'-FL-d(TTGGTGATCC)-d(GGATCACCAA)-TR-3' and 9  $\mu\text{g}$  of  $\lambda$  phage DNA in 1.75 mL of the same buffer pre-equilibrated at 16.2 °C. Fluorescence was continuously monitored by recording the number of photons emitted over 1-s intervals. Solid lines drawn through each set of data points were determined by nonlinear least-squares fitting of the integrated second-order (association) and first-order (dissociation) rate equations.

different temperatures. Method 1 was used for recording the dissociation measurements. The resulting association and dissociation rate constants for the 10-mers and 20-mers are plotted in Figure 6 as  $\log k$  versus  $1/T$  (Arrhenius plots). Also plotted in Figure 6 are the lines calculated by least squares which best fit the data sets. Activation energies,  $E_{\text{act}}$ , and the natural logarithms of the collision factors,  $A$ , determined from the least-squares fits are listed in Table IV.

## DISCUSSION

Placing combinations of fluorescent labels on the termini of complementary oligonucleotides, in the manner used here, provides a sensitive method for monitoring DNA hybridization in solution. The sensitivity of this method is demonstrated by the ability to record fluorescence-based melting curves routinely at oligomer concentrations 2 orders of magnitude below the concentrations achievable with absorbance-based melting curves. In Figure 4, the absorbance data for the 10-mers stop at 0.3  $\mu\text{M}$  while the fluorescence data continue to 1 nM. Absorbance measurements become more sensitive as the oligomer length increases, but the 20-mer absorbance data still stop at a strand concentration 60-fold higher than the



Table III: Dissociation Rate Constants of 10 nM 5'-FL-d(TTGGTGATCC)-d(GGATCACCAA)-TR-3' Observed at Different Concentrations of Excess Unlabeled d(TTGGTGATCC) at 30.5 °C<sup>a</sup>

method	[d(TTGGTGATCC)] (μM)	$k_{-1}$ (s <sup>-1</sup> )
1	1.0	0.0122
1	3.2	0.0108
1	10.0	0.0101
2	1.0	0.0108
2	3.2	0.0112
2	10.0	0.0109

<sup>a</sup> Refer to the text for a description of the two methods used to determine  $k_{-1}$ .

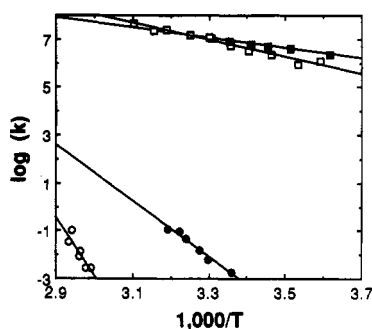


FIGURE 6: Arrhenius plot for association and dissociation of 5'-FL-d(TTGGTGATCC)/d(GGATCACCAA)-TR-3' (solid squares and solid circles, respectively) and 5'-FL-d(AGATTAGCAG-GTTTCCACC)/d(GGTGGGAAACCTGCTAATCT)-TR-3' (open squares and open circles, respectively) in 1 M NaCl/10 mM NaH<sub>2</sub>PO<sub>4</sub>, pH 8.0, containing 5–10 μg of λ phage DNA/mL as carrier. Rate constants were determined from nonlinear least-squares fits of the integrated rate equations to the association and dissociation curves recorded at different temperatures.

Table IV: Activation Energies,  $E_{act}$ , and Natural Logarithms of Collision Factors,  $A$ , Determined from Arrhenius Plots of Dissociation and Association Rate Data

	10-mers	20-mers
dissociation		
$E_{act}$ (kcal/mol)	53.4 ± 7.9	112 ± 57
$\ln A$	84 ± 13	163 ± 86
association		
$E_{act}$ (kcal/mol)	9.94 ± 0.79	16.4 ± 1.8
$\ln A$	32.7 ± 1.4	43.3 ± 3.0

corresponding fluorescence data. As the length of the DNA strands increases, the increased absorbance per strand must increase, eventually to a point in which absorbance measurements become more sensitive than the measurement of fluorescence from a single fluorophore. However, the ability to derive thermodynamic data from melting curves is limited to relatively short oligomers since the concentration dependence of the  $T_m$  becomes smaller as the number of nucleotides per strand increases. This places a practical limit on oligomers which may be studied by absorbance hypochromicity well below the 20-mer length. This can be seen from the erroneous value of  $\Delta G^\circ_{298}$ , determined from the 20-mer absorbance melting curves, listed in Table I, when compared to the predicted value (see discussion below). The ability to record fluorescence melting curves at 1 nM 20-mers permitted a larger change in  $T_m$ 's to be measured, thereby providing a reasonable value for  $\Delta G^\circ_{298}$ . It may be noted that the lower concentration limit of fluorescence-based melting curves is due not to the lack of fluorescence intensity but instead is due to the rate of the bimolecular association reaction. Below 1 nM oligomer concentration, the recording of a complete melting curve requires more than 1 day in order to maintain

the hybridization reaction near equilibrium while slowly changing the temperature.

The reduced fluorescence intensity of double-stranded oligomers relative to single-stranded oligomers, resulting from quenching interactions between the terminal fluorophores in double-stranded complexes, occurs in homogeneous solution. Since the fluorescence measurements are performed on DNA in solution, perturbations of the equilibria caused by the introduction of solid phases, as required by other high-sensitivity detection methods, are not an issue. The introduction of the fluorescent labels, however, does raise questions about the interpretation of the physical constants derived from the fluorescence measurements and listed in Table I. Qualitatively, melting curves recorded by fluorescence and absorbance are similar. Fluorescence-based melting curves appear to have the same sigmoidal temperature dependence in the region of the  $T_m$  as do absorbance-based melting curves. Like absorbance-based melting curves, fluorescence melting curves showed little hysteresis in the region of the transition between single- and double-stranded DNA, but hysteresis in fluorescence quenching did become significant at high temperatures. Examination of the fluorescence dependence of FITC-labeled single-stranded DNA (Figure 2) showed that the high-temperature hysteresis results from a temperature dependence of the single-strand fluorescein emission. A linear correction of the melting curves for the fluorescein temperature dependence resulted in considerable decrease of the hysteresis. It may be noted that although the absorbance or fluorescence of a DNA sample is expected to become constant beyond the melting transition, this is not entirely realized even in absorbance melting curves due to continued randomization of the single-stranded DNA coil with increasing temperature. However, the majority of the absorbance or fluorescence change occurs within a few degrees on either side of the  $T_m$ , and the temperature dependence of the unhybridized strands within this narrow region should contribute little to the total change. In fact, a comparison of the uncorrected and corrected fluorescence data ( $1/T_m$  versus  $\log[S_1]_0$ ) showed that the two data sets were not statistically different. This simplifies the measurement of  $T_m$  values since the determination of the single-stranded DNA temperature dependence and correction of the melting curves are unnecessary when curve-fitting is confined to the transition region. At higher  $T_m$  values than those observed here, the temperature dependence of the single-strand fluorescence in the transition region may become substantial and require correction.

If fluorescence-based melting curves are to be used for thermodynamic studies of DNA, qualitative agreement between absorbance- and fluorescence-based melting curves is not enough. Fluorescence quenching associated with hybridization must be proportional to the number of base pairs formed and, therefore, the absorbance hypochromicity, for conventional equilibrium analysis. Proportionality is expected to be true within the scope of the simplest model of hybridization, the "all-or-none" or "two-state" model, where the complementary strands are either completely hybridized (all possible base pairs are formed) or completely dissociated. The situation becomes more complicated when partially hybridized complexes are allowed, as in the "zipper" model of hybridization (Applequist & Damle, 1963, 1965). The possible base pairs allowed by the "zipper" model are shown in Figure 7 for a pair of 5-mer oligonucleotides. Each row represents the structures for a fixed number of base pairs, and the fraction of the possible base pairs formed is listed together with the fraction of the structures which have the fluorophore-labeled terminal base

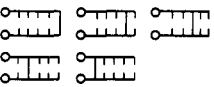
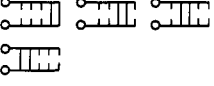
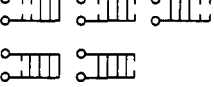
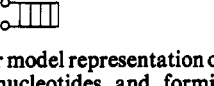
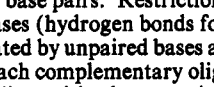
Base Pairs Formed	Allowed Structures	% Pairs Formed	% Quenching
1		20	20
2		40	25
3		60	33
4		80	50
5		100	100

FIGURE 7: Zipper model representation of complementary oligomers containing five nucleotides and forming between one and five hydrogen-bonded base pairs. Restrictions on the allowed structures are that paired bases (hydrogen bonds formed between nucleotides) may not be separated by unpaired bases and staggered structures are not permitted. Each complementary oligomer strand is represented by a horizontal line with short vertical lines representing each nucleotide. Base pairing is indicated by a vertical line connecting the two oligomers. The fluorescent labels are represented by circles. Percent quenching is calculated as the percentage of the allowed structures which have paired nucleotides adjacent to the fluorescent labels.

pair hybridized. Assuming that the terminal bases must be paired to permit efficient quenching interactions between the fluorophores, the fluorescence quenching is always proportionately less than the fractional base pairing, except for the single-base-paired, fully paired, and unpaired structures. These latter two states, of course, represent the allowed states of the "all-or-none" model. At temperatures near the  $T_m$ , then, the "zipper" model predicts a lesser proportion of fluorescence quenching (higher fluorescence intensity of the fluorescein label) than absorbance hypochromicity, leading to the determination of a lower apparent  $T_m$  from fluorescence melting curves. This analysis is oversimplified, however, because of two factors: (1) collisional rates between the terminal fluorophores may be significant when the terminal base pair is not formed, and, therefore, quenching may need to be weighted for the number of bases unpaired at the labeled end of the oligomers; (2) absorbance hypochromicity is not linear with the number of base pairs formed but is greater per base pair as the number of base pairs increases (Rich & Tinoco, 1960). Depending upon the weighting of fluorescence quenching with the number of unpaired bases at the labeled termini, greater or lower quenching relative to hypochromicity can be predicted.

For some complementary oligomers, a high degree of base pairing is also possible in staggered structures (terminal nucleotides not aligned with one another). Both absorbance hypochromicity and fluorescence quenching would be reduced in these structures due to the lower number of base pairs formed and the larger distance separating the terminally attached fluorophores. The effect of the less stable staggered structures is minimized in thermodynamic measurements if melting curves are initiated at the high-temperature extreme (strands completely denatured), as done here. Maintaining the system close to equilibrium as the temperature is lowered favors formation of the more stable fully base-paired structure. In order to obtain reliable thermodynamic information, however, sequences which allow staggered structures of stability similar to the fully base-paired structure should be avoided. The presence of such structures would be indicated by substantially less quenching than that observed in perfectly

aligned strands (near 80% quenching for the fluorescein/Texas Red fluorophore pair).

Quantitative comparisons of the 10-mer absorbance- and fluorescence-based melting curves do show good agreement as demonstrated by measurements of both the widths of the transition regions and the  $T_m$  values. In Table II, the averages of  $\Delta t$ 's recorded over the forward and reverse temperature sweeps were within 1 °C for the absorbance and fluorescence melting curves at two different concentrations compared. A comparison of the  $T_m$  values plotted in Figure 4 determined by both fluorescence and absorbance on the fully labeled 10-mers (5'-fluorescein on one strand, 3'-Texas Red on the complement) showed no statistical difference between the absorbance and fluorescence data sets. These comparisons indicate that the interaction between the two terminally attached fluorescent labels varies with strand separation in the same manner that absorbance hypochromicity does. Since the presence of significant amounts of partially denatured DNA should cause detectable discrepancy between the fluorescence- and absorbance-derived  $T_m$  values, we are led to the conclusion that the "all-or-none" model of DNA hybridization provides an adequate description of short oligomer hybridization. This is consistent with the findings of Applequist and Damle whose population analysis of 11-mer polyadenylic acid at low pH showed that the large majority of the structures either were completely nonbonded or contained two or fewer nonbonded bases (Applequist & Damle, 1965).

The above discussion demonstrates that the thermodynamic values determined from fluorescence melting curves of oligomers are equivalent to values determined from conventional hypochromicity measurements. However, how does the presence of covalently attached fluorophores alter the thermodynamic values relative to unlabeled DNA? The effect of each label on the stability of double-stranded 10-mers may be ascertained from the data plotted in Figure 4 and the thermodynamic constants computed from these data and listed in Table I. Short complementary strands of DNA were used in this study in order to emphasize the effect of labels attached to the DNA. The effect of the 5'-terminal fluorescein label can be seen by comparing the data sets represented by the open triangles (both strands unmodified) and open circles (one strand unmodified and the other strand 5'-labeled with fluorescein) in Figure 4. Certainly the label has a significant effect upon the hybridization equilibrium, as judged from the different slopes and intercepts of the least-squares lines drawn through the two data sets. In fact, the presence of a single fluorescein label significantly decreased both the  $\Delta H^\circ$  and  $\Delta S^\circ$  of hybridization, as seen in Table I. Comparisons of the  $\Delta G^\circ_{298}$  showed that the fluorescein label stabilized the hybridized strands by 3.5 kcal/mol. A binding interaction between the terminal fluorescein and the DNA double helix is indicated by the lower enthalpy change when the label is present as well as by the lower entropy change. The destabilizing change in the entropy may result from a greater restriction in the motion of the fluorescein label in the double-stranded state resulting from stronger interactions with base-paired nucleotides relative to unpaired nucleotides.

It may be noted that the overall stabilizing effect of the terminal fluorescein label observed here is opposite to the overall destabilizing effect observed previously for fluorescein attached to a central base position of an eight-nucleotide-long DNA oligomer (Telser et al., 1989). In that study, the centrally located FTIC was linked to the oligomer via a 5-[2-(*N*-2-aminoethyl)]propionamide modification of deoxyuridine, demonstrating that the particular method of linking the



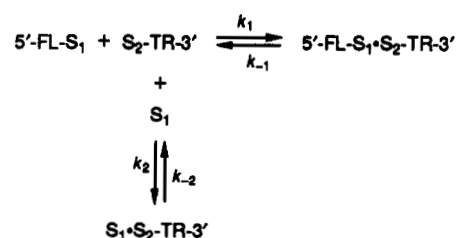
fluorophore to the DNA has a profound effect upon the interaction of the label with the single- and double-stranded states of the DNA.

Also in contrast to the effect of the terminal FITC label is the effect of the Texas Red label. A small favorable enthalpy change for hybridization was observed; however, the decreased entropy change resulted in almost no change in the  $\Delta G^\circ_{298}$  of the oligomer. This can also be seen in Figure 4 where the  $1/T_m$  values of the 10-mer pair containing a single Texas Red label as a function of  $\log[S_1]_0$  (solid triangles) are not much altered from the values of the unmodified oligomers (open triangles). When both labels were present, the concentration dependence was more similar to the 5'-FITC-only data than the unmodified DNA data, indicating the interaction of FITC with the DNA strands is the dominant effect. The two labels are not completely independent in their effect on the DNA hybridization, however, as can be seen from the increase in the  $\Delta H^\circ$  and  $\Delta S^\circ$  of hybridization when both labels were present compared to when only the FITC label was present.

Thermodynamic data for fully labeled (5'-FITC on one strand, 3'-Texas Red on the complementary strand) and unlabeled 20-mers are compared on the last two rows of Table I. As noted above, comparisons of the 20-mer data sets show large discrepancies which appear too large to be due to the effects of the labels in view of the 10-mer data. A value for  $\Delta G^\circ_{298}$  can be estimated using nearest-neighbor interactions (Breslauer et al., 1986). These estimates are usually fairly accurate as can be seen by comparing experimental and predicted (last column) values of  $\Delta G^\circ_{298}$  for the unmodified 10-mer in Table I (top row). For the 20-mers, however, the prediction differs greatly from the  $\Delta G^\circ_{298}$  determined from absorbance measurements of the unlabeled 20-mers, but is only 1.5 kcal/mol different from the  $\Delta G^\circ_{298}$  determined from fluorescence measurements of the labeled 20-mers. In fact, the 1.5 kcal/mol difference is the same as the difference between the experimentally determined  $\Delta G^\circ_{298}$  values for the fully labeled and unmodified 10-mers. The erroneous  $\Delta G^\circ_{298}$  determined from absorbance measurements illustrates the advantage of using fluorescence measurements for longer oligomers. This advantage results from the wider concentration range accessible to fluorescence measurements. Looking at eq 6, it may be seen that the dependence of  $1/T_m$  upon  $\log[S_1]_0$  becomes less as the absolute value of  $\Delta H^\circ$  increases. Since  $|\Delta H^\circ|$  increases with oligomer length, the difference between  $1/T_m$  measured at the highest and the lowest oligomer concentrations decreases relative to the error in the  $1/T_m$  measurement. This increases the percentage error in the slope determination, and consequently increases the error in the  $\Delta H^\circ$  and  $\Delta S^\circ$  determined for larger oligomers. The only way to compensate for this is to expand the accessible concentration range, which was achieved here by using fluorescence.

In addition to monitoring hybridization equilibria, fluorescence quenching between terminal fluorescent labels provided a sensitive means for measuring hybridization rates. From the simple one-step dissociation and association scheme shown in Figure 1, first- and second-order rates of dissociation and association are expected and were observed, respectively, for the labeled 10-mers and 20-mers. This is shown in Figure 5 where the fluorescence versus time data were closely fit by their respective first- and second-order integrated rate equations. Together with the linear Arrhenius plots of rate constants determined from these fits (Figure 6), a simple "all-or-none" model for hybridization appears adequate to explain hybridization rates. However, the activation energies of the

Scheme I



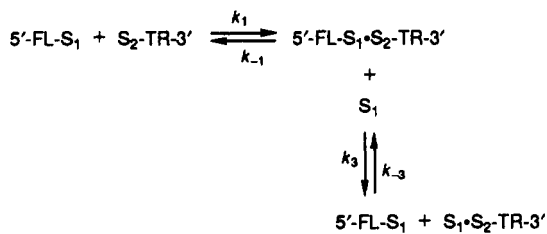
10-mers and 20-mers (Table IV), when compared to their  $\Delta H^\circ$  values determined from the melting curves, provide evidence that a more complex mechanism is operating. For a simple "two-state" or "all-or-none" model, the difference between the activation energy for association and dissociation should equal the enthalpy change. The  $\Delta H^\circ$  values determined by the activation energies are  $-43.5 \pm 8.7$  and  $-96 \pm 59$  (uncertainties are the sums of uncertainties in the activation energies) for the 10-mers and 20-mers, respectively, as compared to the thermodynamically measured  $\Delta H^\circ$  values of  $-71.6 \pm 5.0$  and  $194 \pm 48$ , respectively.

Comparisons of enthalpy changes measured by kinetic and thermodynamic methods are not typically high in accuracy; however, the fairly large difference here supports a more complicated mechanism. Association mechanisms involving nucleation and chain extension steps have been described in detail (Applequist & Damle, 1965; Cantor & Schimmel, 1980). Thus, while intermediately base-paired structures may contribute little to the mass balance at equilibrium, their importance as intermediates in the mechanisms of association and dissociation has a significant effect on the observed kinetics.

The advantages of the fluorescence quenching method in performing association rate measurements arise from the ability to monitor low concentrations of DNA oligomers in solution. The amount of DNA material is conserved, but more importantly, the bimolecular reaction rates can be manipulated to facilitate the rate measurements. By lowering the oligomer concentrations, association rates can be slowed to the point that simple manual or automated mixing techniques can be employed to initiate the reactions without the need to correct for mixing times. For example, in experiments reported here, the addition of one labeled complementary strand to the other was accomplished using an automated syringe which injected one strand over a period of 0.5–2.5 s, depending upon the volume injected and the injection speed selected. At 1  $\mu\text{M}$  concentrations of each 10-mer strand, at 20  $^\circ\text{C}$ , the association is calculated to be half-completed in 0.16 s, which would result in a very large mixing artifact. At 10 nM concentrations of each 10-mer strand, at the same temperature, the reaction is calculated to be half-completed in 16 s, and the mixing artifact is small.

As a first-order reaction, DNA dissociation cannot be manipulated in the same manner by lowering the oligomer concentrations. However, an isothermal label-dilution technique, unique to the labeled oligomers, was used which allows the dissociation rate to be measured well below the  $T_m$  where the rates are low. This technique takes advantage of the dynamic equilibrium of the complementary DNA strands whereby the strands continually undergo dissociation and reassociation. When the labeled complementary strands are at equilibrium, the amount of fluorescence quenching measures the fraction of the strands which are hybridized at any particular moment in time, as determined by the ratio of  $k_1$  to  $k_{-1}$ . If an unlabeled DNA strand ( $S_1$ ) complementary to

### Scheme II



one of the labeled strands, for example, the 3'-Texas Red-labeled strand ( $S_2$ -TR-3'), is then introduced, the unlabeled strand competes with the 5'-FITC-labeled strand ( $S_1$ -FITC- $S_1$ ) for binding to any single-stranded 3'-Texas Red-labeled strand, according to Scheme I. The association and dissociation of  $S_1$  and  $S_2$ -TR-3' are "silent" events since the FITC label is not involved. If  $S_1$  is added in large excess to 5'-FITC- $S_1$ , then single-stranded  $S_2$ -TR-3', formed by dissociation of 5'-FITC- $S_1$ - $S_2$ -TR-3', associates preferentially with  $S_1$ , and the association process governed by  $k_1$  is negligible. The only process observed by monitoring the FITC emission is the dissociation of 5'-FITC- $S_1$ - $S_2$ -TR-3' governed by  $k_{-1}$ .

The above discussion of the dilution technique is valid only in the absence of a second-order strand displacement reaction, shown in Scheme II. With a large excess of added  $S_1$ , strand displacement would produce a pseudo-first-order increase in FITC emission (relief of quenching), as would the first-order dissociation process; however, the observed rate constant would be proportional to the concentration of  $S_1$ . Strand displacement was determined to be negligible in experiments reported here in which the observed rate constant was independent of  $[S_1]$  over a 10-fold concentration range (Table III).

It should be noted that situations may arise in which strand displacement becomes significant. For example, one or both labeled strands might contain single-stranded regions due to differences in strand lengths or mismatched nucleotides, thereby providing nucleation sites for the unlabeled strand. Measuring rates at different concentrations of the unlabeled strand, as shown here, would then serve to determine if strand displacement was significant and would provide a means to study the displacement reaction.

In conclusion, we have demonstrated that the thermodynamics and kinetics of DNA hybridization can be characterized in solution using fluorophore-labeled DNA. This approach permits access to a much wider range of DNA concentrations and eliminates perturbations resulting from the introduction of immobilization supports or solid precipitates. The ability to perform hybridization measurements over a wide range of DNA strand concentrations conserves DNA material, allows longer oligomers to be used for thermodynamic measurements, and allows broad control of DNA association rates. In addition, labeled fluorescent probes provide a unique isothermal method for measuring dissociation rates, also providing broad control of the rates. Such flexibility in selecting association and dissociation rates allows the use of simple injection and mixing methods, as well as the use of detection methods with relatively slow response times. These advantages come with the disadvantage that labels must be attached to the DNA strands, requiring additional synthetic work and altering the properties of the strands to some extent. The alterations become less significant for longer DNA strands and may be accounted for by performing comparative

measurements on labeled and unlabeled DNA. This approach may find importance in studies of the relative properties of related DNA sequences. For example, the destabilization which results from introducing various mismatched bases into positions removed from the labeled termini could be determined. Similarly, the thermodynamic and kinetic properties of various length DNA strands, sharing the same several terminal nucleotides and labels, could be determined relative to one another since the label effects should be constant for the series of oligomers. As a final note, these studies could be extended to investigate the dynamics of individual domains within high molecular weight DNA. It is conceivable that combined oligomer synthesis, restriction cleavage of DNA, and ligation could introduce labeled nucleotides at specific positions within naturally occurring DNA. Fluorescence quenching, as well as fluorescence polarization and lifetime analyses, could then be used to determine localized strand separation and mobility which could be correlated with molecular events that occur in transcription, translation, regulation, and packaging of DNA.

## ACKNOWLEDGMENT

We thank Kenneth Cruickshank and Dan Stockwell for the synthesis of DNA oligomers used in this study. We also thank Eric Ziegel, Vincent Hodgson, and Don Porter for their help and discussions on the statistical analyses reported here.

## REFERENCES

- Appelquist, J., & Damle, V. (1963) *J. Chem. Phys.* 39, 2719-2721.
- Appelquist, J., & Damle, V. (1965) *J. Am. Chem. Soc.* 87, 1450-1458.
- Borer, P. N. (1976) in *Handbook of Biochemistry and Molecular Biology* (Fasman, G. D., Ed.) p 589, CRC Press, Cleveland, OH.
- Breslauer, K. J. (1986) in *Thermodynamic Data for Biochemistry and Biotechnology* (Hinz, H.-J., Ed.) pp 402-427, Springer-Verlag, New York.
- Breslauer, K. J., Frank, R., Blocker, H., & Marky, L. A. (1986) *Proc. Natl. Acad. Sci. U.S.A.* 83, 3746-3750.
- Bush, C. A. (1974) in *Basic Principles in Nucleic Acid Chemistry* (Ts'o, P. O. P., Ed.) pp 91-169, Academic Press, New York.
- Cantor, C. R., & Schimmel, P. R. (1980) *Biophysical Chemistry Part III: The behavior of biological macromolecules*, Chapter 23, Freeman and Company, San Francisco.
- Cardullo, R. A., Agrawal, S., Flores, C., Zamecnik, C., & Wolf, D. E. (1988) *Proc. Natl. Acad. Sci. U.S.A.* 85, 8790-8794.
- Chu, B. C. F., Wahl, G. M., & Orgel, L. E. (1983) *Nucleic Acids Res.* 11, 6513-6529.
- Heller, M. J., & Morrison, L. E. (1985) in *Rapid Detection and Identification of Infectious Agents* (Kingsbury, D. T., & Falkow, S., Eds.) pp 245-256, Academic Press, New York.
- Lakowicz, J. R. (1983) *Principles of Fluorescence Spectroscopy*, p 264, Plenum Press, New York.
- Morrison, L. E. (1987) European Patent Application 232 967.
- Morrison, L. E. (1992) in *Nonisotopic DNA Probe Techniques* (Kricka, L. J., Ed.) pp 311-352, Academic Press, San Diego.
- Morrison, L. E., Halder, T. C., & Stols, L. M. (1989) *Anal. Biochem.* 183, 231-244.
- Patel, D. J., Pardi, A., & Itakura, K. (1982) *Science* 216, 581-590.
- Rich, A., & Tinoco, I., Jr. (1960) *J. Am. Chem. Soc.* 82, 6409-6411.
- Telser, J., Cruickshank, K. A., Morrison, L. E., & Netzels, T. L. (1989) *J. Am. Chem. Soc.* 111, 6966-6976.